Methods 169 (2019) 69–77

Contents lists available at ScienceDirect

Methods

journal homepage: www.elsevier.com/locate/ymeth

Multi-parameter measurements of conformational dynamics in nucleic acids and nucleoprotein complexes

Ivan E. Ivanov[a,b,1], Zev Bryant[b,c,*]

[a] Department of Chemical Engineering, Stanford University, Stanford, CA, USA
[b] Department of Bioengineering, Stanford University, Stanford, CA, USA
[c] Department of Structural Biology, Stanford University School of Medicine, Stanford, CA, USA

ARTICLE INFO

Keywords:
Force spectroscopy
Torque
Rotor bead tracking
Nanopore
Multimodal

ABSTRACT

Biological macromolecules undergo dynamic conformational changes. Single-molecule methods can track such structural rearrangements in real time. However, while the structure of large macromolecules may change along many degrees of freedom, single-molecule techniques only monitor a limited number of these axes of motion. Advanced single-molecule methods are being developed to track multiple degrees of freedom in nucleic acids and nucleoprotein complexes at high resolution, to enable better manipulation and control of the system under investigation, and to collect measurements in massively parallel fashion. Combining complementary single-molecule methods within the same assay also provides unique measurement opportunities. Implementations of magnetic and optical tweezers combined with fluorescence and FRET have demonstrated results unattainable by either technique alone. Augmenting other advanced single-molecule methods with fluorescence detection will allow us to better capture the multidimensional dynamics of nucleic acids and nucleoprotein complexes central to biology.

1. Introduction

Single-molecule measurement methods can provide valuable insights into nucleic acid and nucleoprotein dynamics by observing conformational changes in real time [1–3]. Single-molecule manipulation methods such as magnetic and optical tweezers can further apply perturbations in the form of force or torque to probe energetics and reaction mechanisms [4]. While molecular dynamics are highly multidimensional, single-molecule techniques are limited in the number of conformational degrees of freedom that can be observed (Figure 1A-B). In optical tweezers and magnetic tweezers, for example, the dynamics of nucleic acids and associated proteins are typically inferred from changes in the end-to-end extension of a nucleic acid tether. Alternatively, molecular domains undergoing large structural rearrangements can be directly tagged using fluorescent dyes or nanoparticle probes. FRET measurements of conformational changes are commonly employed in observing dynamic transitions between states (Figure 1B) [5,6], and non-bleaching scattering probes have been used to elucidate the mechanisms of molecular motors [7–9].

Measuring a single degree of freedom may capture the key conformational change in a system of interest, but is insufficient for understanding the dynamic series of conformational rearrangements expected for cellular machines. Single-molecule methods can be extended to collect information on multiple mechanical degrees of freedom simultaneously or to enable more versatile manipulation of the system of interest [10,11]. Magnetic tweezers and optical trapping techniques have also been combined with fluorescence and FRET to detect compositional (binding, dissociation, oligomerization) and conformational changes in macromolecular complexes in addition to monitoring mechanical events (Figure 1C) [12,13]. A prior review by Cordova et al. describes how these methods have been combined with fluorescence detection [12]. Here we will overview other advanced multi-parameter single-molecule techniques and will present recent discoveries enabled by such multimodal tools. Dynamic information on multiple conformational degrees of freedom can be used to develop and test mechanistic and structural hypotheses.

2. Advanced single-molecule methods

Single-molecule techniques are undergoing continual improvement. The spatiotemporal resolution of mechanical measurements is fundamentally limited by Brownian fluctuations of the probe, commonly a

* Corresponding author.
E-mail address: zevry@stanford.edu (Z. Bryant).
[1] Present address: Chan Zuckerberg Biohub, San Francisco, CA, USA

https://doi.org/10.1016/j.ymeth.2019.06.019
Received 7 March 2019; Received in revised form 15 June 2019; Accepted 18 June 2019
Available online 19 June 2019

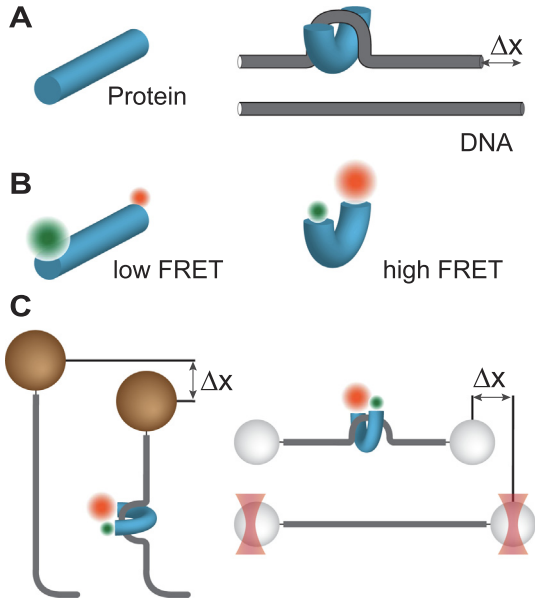

Figure 1. Dynamics of nucleoprotein complexes observed in single-molecule experiments. (**A**) A hypothetical example of a protein that undergoes conformational change upon binding DNA. A bend in the DNA structure leads to contraction of its end-to-end extension. (**B**) Conformational changes in the protein structure can be observed using FRET. (**C**) Structural dynamics in both the protein and the DNA substrate can be observed by magnetic tweezers (left) or optical tweezers (right) combined with FRET.

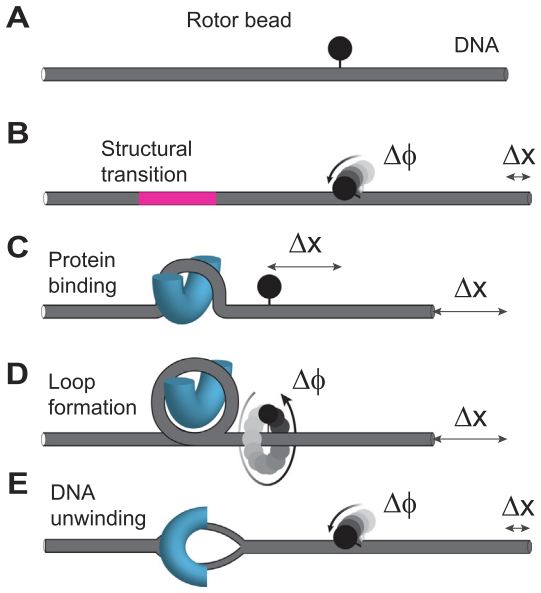

Figure 2. Rotor bead tracking measures changes in DNA twist and extension. Angular tracking of a nanoparticle attached to the side of the DNA (**A**) can report on changes in DNA twist (Δφ) and extension (Δx) arising from structural transitions in DNA (**B**), protein binding (**C**), formation of loops in DNA (**D**), or unwinding of the DNA double helix (**E**). Extension changes can be measured from the end-to-end extension of the DNA or from the linear translation of the rotor bead.

spherical bead, provided that the instrument noise floor (e.g. due to drift or vibration) is sufficiently low [14]. Decreasing the size of the probe or increasing the stiffness of the attached molecular tether allow for faster averaging of the Brownian fluctuations and can reveal smaller and faster conformational changes in biological macromolecules. Distance measurements via single-molecule FRET [5,6] are fundamentally limited by the photon statistics of fluorescence emission. While improved signal-to-noise can be achieved using higher excitation intensities, in practice irreversible dye photobleaching imposes a trade-off between signal-to-noise and observation time. The ability to detect the binding of a single fluorophore may further be limited by fluctuating background intensity from other diffusing fluorophores. New biophysical tools have pushed the limits of resolution by using smaller probes, local tethering, or confined fluorescence excitation. Important efforts to advance the state of the art in single-molecule measurement by extending the resolution of established methods such as optical trapping have been reviewed elsewhere [1,3,15,16]. In this section, we will focus on advanced methods that also provide additional conformational degrees of freedom or exploit new measurement modalities, and we will discuss the opportunities these methods offer for the study of nucleic acids.

Rotor bead tracking (RBT) was initially developed as an extension of optical tweezers enabling combined detection of changes in extension and twist in DNA (Figure 2). In RBT, the rotational motion of a submicron sphere (the rotor bead) attached to the side of the DNA molecule (Figure 2A) provides information on angular changes. Structural changes in DNA often exhibit interplay between twist and extension (Figure 2B). For example, Gore et al. showed that DNA overwinds when stretched [17]. RBT enabled precise measurements of DNA physical properties and observations of DNA structural transitions under torque [18]. A large array of cellular processes can also be dissected though the lens of changes in twist and extension of biological filaments (Figure 2C-E) [19]. Protein binding frequently leads to bending of the DNA double helix or sequestration of DNA contour length (Figure 2C). Wrapping of DNA around protein complexes such as histones (Figure 2D) can further trap DNA supercoils and lead to compensatory change in superhelical density in the rest of the topologically constrained region of the genome. Topoisomerases permanently alter the linking number of a closed circular piece of DNA and serve to relax positive and negative spikes in DNA superhelical density, which arise, for instance, during transcription [20]. Changes in DNA twist can also be observed as the double helix is unwound within nucleoprotein complexes (Figure 2E). While many DNA transactions involve changes in both extension and twist, the signal may be easier to measure in one of the two coordinates [21,22]; collecting information on both coordinates at once can resolve ambiguities and test specific structural hypotheses.

RBT is now commonly applied in magnetic tweezers setups (Figure 3A) [23–27], rather than the original optical tweezers implementation. This approach has been used to explore sequence-dependent structural transitions in DNA, deriving quantitative thermodynamic models for the transition of $(GC)_n$ repeats into Z-DNA, the melting of $(AAT)_n$ regions, and the formation of helical structure in mismatched DNA bubbles under torque [25,26]. These studies identified cooperative transitions in short sequence motifs and estimated boundary penalties at the junction of structural domains. Such localized structural transitions may be triggered during torque-generating biological processes such as replication or transcription [19].

Lebel et al. developed high-resolution gold rotor bead tracking (AuRBT) by replacing the ~ 300 – 500 nm rotor beads used in previous studies by gold nanoparticles with diameters of ~ 80 – 140 nm [24]. Reducing the hydrodynamic drag of the measurement probe allowed faster averaging of the thermal noise and enabled twist and torque measurements at temporal resolutions several orders of magnitude higher than competing techniques [24,28–31]. In AuRBT, the rotor bead is observed via evanescent darkfield imaging, and stable high-resolution extension measurements can also be obtained from the intensity of the rotor bead in the evanescent field.

RBT has been applied to studying the mechanisms of DNA-associated motors including DNA gyrase. By tracking simultaneous changes in twist and extension during processive DNA supercoiling by gyrase, Basu et al. identified an unanticipated dominant ATP waiting

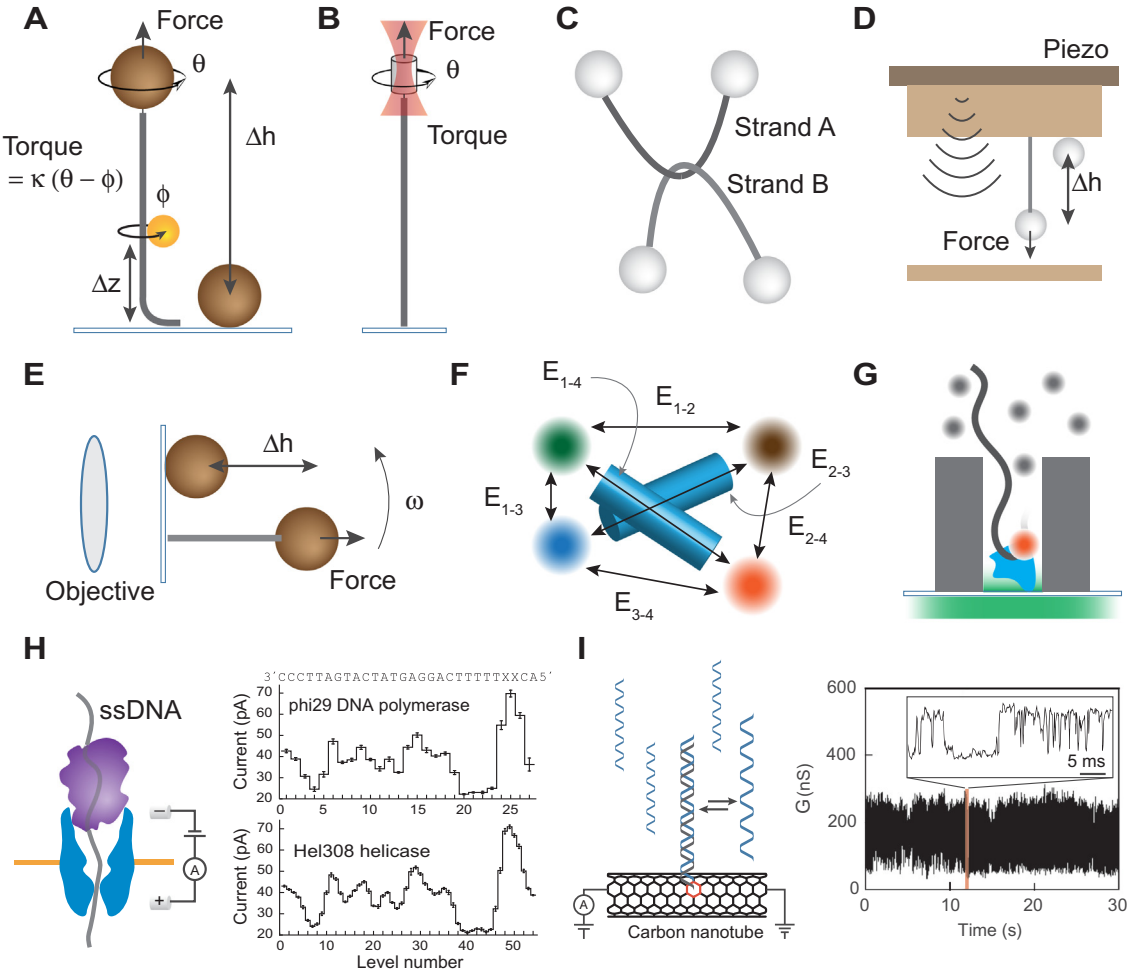

Figure 3. Advanced single-molecule methods. (**A**) Rotor bead tracking applied in magnetic tweezers [23,24,100]. The magnetic bead is used to apply force on DNA and can be rotated to change the DNA twist. The applied torque is measured from the difference in angle of the magnetic bead (θ) and the rotor bead (φ) using the calibrated torsional stiffness (κ) of the DNA segment between them. Changes in DNA extension can be measured from the intensity of the rotor bead in an evanescent field (Δz) or from the height of the magnetic bead above a reference bead (Δh). (**B**) Optical torque wrench [31]. Trapping a cylindrical quartz nanoparticle allows application of force and changing the DNA twist by rotating the polarization of the trapping beam. Torque on the DNA is measured based on the imparted change in angular momentum on the trapping beam. (**C**) Quad optical trap [35]. Independent manipulation of two DNA strands or cytoskeletal filaments can be achieved by trapping four beads. (**D**) Acoustic force spectroscopy [44,45]. A piezoelectric transducer creates a standing wave which can exert forces on densely-spaced beads. Changes in extension of DNA attached to the microspheres (Δh) can be measured using a refence bead. (**E**) Centrifugal force spectroscopy [46]. Massively parallel DNA tweezers can also be made by spinning a simple microscope at angular velocity ω. Changes in DNA extension (Δh) are measured as in previous techniques. (**F**) Four-color FRET [55]. Six interdye distances (E_{i-j}) can be measured by consecutive excitation of the blue, green and red fluorophores. (**G**) Zero-mode waveguides [60,62]. Subwavelength cylindrical holes in a metallic layer are used to attenuate propagating light. Evanescent excitation of zeptoliter (10^{-21} L) volumes inside the chambers enables detection of single fluorophores at micromolar dye concentrations. (**H**) Nanopore tweezers [67–69]. Left: Steps of motor proteins controlling the passage of ssDNA through a nanopore under applied voltage can be observed based on changes in current as ion flow through the nanopore is affected by the DNA bases [75]. Right: Sequence-dependent changes in current level are detected for the Φ29 DNA polymerase (top) and the Hel308 helicase (bottom). Two distinct current levels are observed for translocation of each single nucleotide, suggesting ~40 pm extension resolution in detecting enzymatic substeps. (**I**) Single-walled carbon nanotube field-effect transistor [78]. Left: A 10 bp ssDNA oligonucleotide is attached to a single defect in the carbon nanotube [78]. Hybridization of the complementary strand changes the electrostatic potential around the defect site and alters the conductance (G, in nanosiemens) of the nanotube. Right: Rapid strand exchange with 1 μM pool of the complementary strand is detected at high signal-to-noise and high temporal resolution. Data are collected at 33 °C.

intermediate [23]. A series of studies identified enzyme substates with characteristic DNA conformations, and produced a detailed description of the gyrase mechanochemical cycle [23,24,27,32]. Combined angle and extension measurements using RBT in an optical tweezers implementation have also been used to study the mechanism of DNA packaging and subunit coordination of the Φ29 viral packaging motor [33]. The authors discovered that Φ29 rotates the DNA molecule to preserve protein-DNA contacts during packaging, and proportionally decreases the step size and DNA rotation as the viral capsid is filled and backpressure increases. The measurement of DNA rotation was instrumental in identifying the mechanism of subunit coordination and symmetry breaking in this pentameric ATPase motor.

A range of other modifications of optical tweezers have further extended the capabilities of the technique. An optical torque wrench was developed by using an optically anisotropic cylinder instead of the common polystyrene or other isotropic microspheres (Figure 3B) [31]. The cylinder can be rotated by changing the polarization of the trapping laser to apply torque on the attached filament. The technique was applied to study transcription by the *E. coli* RNA polymerase under assisting and opposing torque, highlighting how dynamic changes in superhelical density of the genome regulate the motor activity [34]. Implementations of optical tweezers where three or more beads are simultaneously trapped have also been described (Figure 3C) [35,36], with applications involving manipulating more than one DNA molecule

or cytoskeletal filament [37,38].

Magnetic tweezers and RBT can be extended to measurements on multiple molecules at a time. However, interactions of neighboring magnetic beads and overlap of the diffraction patterns used to measure bead displacements impose a limitation on the maximum surface density achievable by random attachment. Using patterned deposition of surface attachment sites on a regular 10 μm grid, De Vlaminck et al. showed simultaneous tracking of 450 beads [39]. Parallel manipulation of optically trapped beads has also been demonstrated using nanophotonic devices [40,41] or holographic optical traps [42,43], and shows promise for making high-throughput nucleic acids measurements. Massively parallel force spectroscopy tools have been developed based on acoustic (Figure 3D) [44,45] or centrifugal (Figure 3E) [46] forces, which do not rely on magnetic beads, and thus facilitate placing tethers at higher density. These methods may further provide increased range, stability, and/or response times compared to currently available techniques. Combinations of optical trapping and acoustic force spectroscopy [47] or magnetic tweezers [48] have also been reported. Such tools expand our ability to probe biological systems and allow us to make statistical measurements based on single-molecule data.

Fluorescence detection of protein conformational changes has been advanced by the development of multicolor FRET (Figure 3F) [49,50]. Three-color single-molecule FRET was first reported in 2004. In combination with alternating laser excitation, the technique was able to report independently on three interdye distances [51–54]. Later the Hohng group reported the development of four-color FRET, which allowed measurement of six interdye distances [55]. Multicolor FRET assays have been used to study structural dynamics of the ribosome [56,57], single-stranded DNA binding protein [58], and RecA-mediated DNA strand exchange [55], and have also been combined with optical tweezers [59].

Fluorescence measurements can be hampered by high fluctuating background when a diffusing labeled species must be used at moderate concentrations, for example because of modest affinity for the observation site. Zero-mode waveguides (Figure 3G) confine fluorescence excitation to volumes as low as zeptoliters, and enable observation of single molecule binding events against the background of 100 – 1000 nM fluorophores in solution [60]. The technology was first refined for DNA sequencing applications [61], but has also been repurposed for making biophysical measurements [62,63]. It has been applied extensively in dissecting translation dynamics at physiological ligand concentrations [64], for example monitoring the number of tRNAs simultaneously bound to the ribosome and showing that having two tRNAs bound occurs only transiently [63]. An alternative technique reducing the imaged volume is Convex Lens-Induced Confinement (CLIC) [65], which deforms the imaging chamber to decrease its depth to 5 – 500 nm. CLIC enables highly parallel fluorescence measurements of single molecules without requiring surface attachment, and has been applied to studying transitions in supercoiled DNA molecules [66].

Other advances in next-generation sequencing technologies have also led to new ways of making biophysical measurements. Nanopore sequencing, for example, can reveal sub-base pair steps in DNA processing enzymes (Figure 3H) [67–70]. In nanopore sequencing, an external voltage is used to thread a segment of single-stranded DNA through a solid-state or biological pore. As the DNA passes through the constriction, sequence-dependent changes in current are detected. Successful versions of the technique also use a DNA motor to slow down passage of the nucleic acid through the constriction for improved reading of the DNA sequence [71]. DNA translocation is thus directed by the mechanochemistry of the motor and enzymatic steps can be observed with sub-Ångstrom resolution, with Brownian fluctuations averaged over quickly due to the short DNA tether length between the enzyme and the constriction where the current blockage occurs. This assay, called SPRNT, has enabled detailed kinetic analysis of DNA processing by the Φ29 DNA polymerase [72–74] and the helicase Hel308 [75,76], and may be extended to other molecular motors such as the machines behind transcription [77] and translation.

Another intriguing very high spatiotemporal resolution single-molecule biophysical method is based on carbon nanotubes which act as field-effect transistors (Figure 3I). The conductance of single-walled carbon nanotubes varies strongly with the local charge density. A single point defect in the nanotube can be used to covalently attach molecules at that site, converting the device into a label-free single molecule detector. Sorgenfrei et al. observed hybridization of a 10 bp segment of DNA with a bandwidth of 4 kHz, which could be extended to over 10 kHz [78]; notably this study also made used of precise variable temperature control, which is rarely incorporated in single-molecule experiments. In a later study, Choi et al. attached a lysozyme to a carbon nanotube device and observed processive hydrolysis steps by the enzyme, as well as nonproductive domain fluctuations [79]. This method shows promise for observing detailed single-molecule nucleic acid dynamics on timescales that are generally inaccessible to optical and mechanical approaches.

3. Methods combining mechanical perturbation and fluorescence detection

Combining different single-molecule methods in the same assay can leverage their unique strengths and provide high-resolution information on a larger number of conformational degrees of freedom. Several groups have combined optical tweezers or magnetic tweezers with fluorescence and FRET to detect local structural and compositional changes under controlled mechanical perturbations. Early work in the field primarily used the tweezers for force application – high-resolution extension measurements were not made, and instead fluorescence was used as a sensitive reporter of changes in the system under observation. One challenge in combining optical tweezers with fluorescence arises from accelerated dye photobleaching as fluorophores in the excited state absorb infrared photons from the high-power trapping laser [80]. The problem can be circumvented by using long DNA tethers to spatially separate the fluorophores and the optical trap (at the expense of compromised spatiotemporal resolution for extension measurements [14]) or by interlacing the trapping and excitation lasers as first demonstrated by Lang and coworkers [81].

A pioneering implementation of optical tweezers and fluorescence used a custom fabricated quartz pedestal for prism-type total internal reflection (TIR) illumination of fluorophores on DNA suspended in a dual-beam optical trap (Figure 4A), with which Harada et al. observed sequence-dependent binding dynamics of fluorescently-labeled RNA polymerase under tension [82]. Subsequent iterations of the technique utilized objective-side TIR illumination of fluorophores at the base of a surface-bound DNA tether (Figure 4B) [83–85]. This technique was used to observe transitions between the folded and unfolded state of a FRET-labeled DNA hairpin under applied force [84] and transitions between stacking isoforms of the Holliday junction using two- and three-color FRET [59,85]. More recently, optical tweezers force-FRET assays have been applied to study the sliding mechanism of the single-stranded DNA binding (SSB) protein [86] and sequence-dependent asymmetric DNA unwrapping from the nucleosome [87].

Epifluorescence excitation combined with dual-beam optical tweezers has been powerful in studying DNA structural transitions under tension (Figure 4C) [88]. This experimental geometry is particularly applicable when the dye labels undergo fluorescence enhancement upon binding DNA or if the labeled probe has high affinity to DNA and can be introduced at low concentration to prevent background fluorescence. Wuite and Peterman and coworkers visualized single-stranded regions in DNA undergoing the overstretching transition using intercalating DNA dyes [89]. In a follow-up study, the group also identified a “hyperstretched” structure of DNA in which such dyes have a reduced affinity [90]. In torsionally constrained DNA, the authors showed bubble formation before the overstretching transition using a GFP-labeled replication protein A reporter, suggesting that such unfavorable

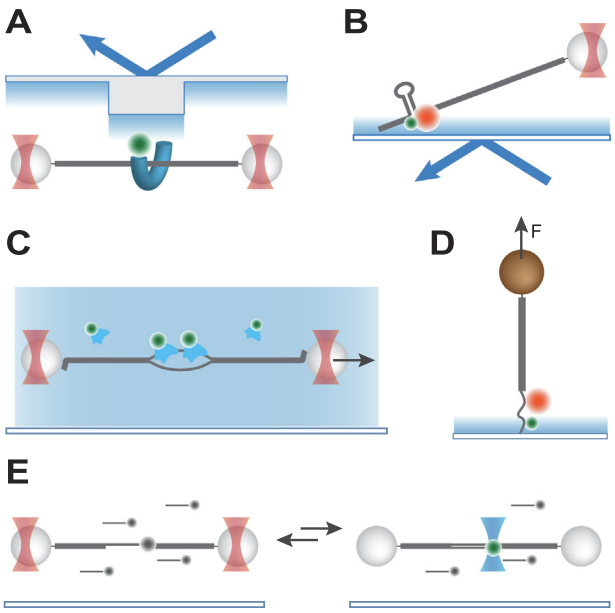

Figure 4. Combining optical and magnetic tweezers with fluorescence. (**A**) Custom-fabricated quartz pedestals are used to create evanescent wave illumination (blue gradient) that selectively excites fluorophores on DNA suspended in a dual-beam optical trap [82]. (**B**) Objective-side TIR illumination is used to excite fluorophores on a hairpin at the base of a DNA tether attached to the surface [83,84]. (**C**) Epifluorescence illumination is used to image fluorophores on a long DNA tether [88]. (**D**) TIR illumination excites fluorophores at the base of a DNA tether stretched using magnetic tweezers [94,100,110]. (**E**) The optical trap and confocal fluorescence excitation are interlaced to prevent accelerated photobleaching of the fluorophores [96]. This technique can use relatively short DNA tethers, facilitating high-resolution extension measurements.

changes in twist density are compensated by the larger extension of single-stranded DNA at high force [91]. Very recently, the combination of optical tweezers with confocal imaging was used to study binding and cleavage of the Cas9 RNA-guided nuclease under tension, revealing mechanically-induced binding at off-target sites [92].

Force-FRET assays have also been implemented in magnetic tweezers, which are readily combined with fluorescence by exciting fluorophores near the surface using total internal reflection illumination [93]. Shroff et al. described the first reported implementation of magnetic tweezers combined with single-molecule FRET, and demonstrated changes in FRET under applied force of a DNA-based molecular force sensor (Figure 4D) [94]. Long et al. used FRET to detect the unfolding of G-quadruplexes under force [95]. Here FRET provided a much stronger signal compared to the expected ~3 nm change in extension upon transition between the folded and unfolded state of the structure.

Multimodal high-resolution extension and FRET measurements in optical tweezers have been achieved using interlaced confocal excitation (Figure 4E) [81,96]. By quickly switching between the fluorescence excitation and the optical trap, dye photobleaching is reduced without allowing the beads to escape the optical trap. These assays achieve high spatiotemporal resolution by using a dual-beam [97] configuration and shorter DNA tethers, reducing sources of noise and drift present in previous studies. Precision instruments combining optical tweezers or magnetic tweezers with fluorescence are usually custom built, although detailed protocols and software for their construction, calibration, and operation are available [15,16,98–102]. Commercial setups combining optical trapping and fluorescence have also recently appeared on the market [103].

4. High-resolution multi-parameter methods

High-resolution optical tweezers combined with fluorescence have been used to investigate a number of biological systems. Comstock et al. used this technique to relate different modes of DNA unwinding to the oligomeric and conformational state of the UvrD helicase, responsible for nucleotide excision and methyl-directed mismatch repair (Figure 5A) [104]. Previous biochemical studies had identified that UvrD dimers or higher oligomers are required for processive double-stranded DNA unwinding [105]. The authors measured changes in extension as UvrD unwinds a DNA hairpin incorporated in the tether and identified two types of DNA unwinding activity – “frustrated” and “long-distance”. The frustrated activity was characterized by repeating back-and-forth translocation in which less than 20 bp of DNA are unwound, while the long-distance activity resulted in processive unwinding of more than 20 bp of DNA with less frequent reversals in direction. By counting the number of photobleaching events of fluorescently-labeled UvrD helicases, the authors proposed that the two DNA unwinding modes correlate with the monomeric and multimeric state of the enzyme, respectively. UvrD monomers further exist in two conformational states, suggesting a mechanism for switching direction without dissociating from the DNA substrate. By labeling UvrD with a FRET dye pair, the DNA unwinding and rezipping activity of UvrD monomers were shown to correlate with the closed and open conformation of the helicase. These different unwinding modes of UvrD may be employed during distinct DNA repair processes carried out by the enzyme.

High-resolution optical trapping and FRET has also been applied in studying different binding modes of the single-stranded DNA binding (SSB) protein (Figure 5B). SSB wraps ssDNA to protect it from nucleolytic and chemical damage during DNA replication, recombination, and repair processes. By unravelling single SSB-ssDNA complexes under force, Suksombat et al. identified four discrete binding states and suggested the most likely geometry of DNA wrapping around the protein subunits based on high-resolution extension measurements of the sequestered DNA contour [106]. The force perturbation additionally allowed the authors to reconstruct the energy landscape of SSB binding in each of the binding modes. Fluorescent labeling of SSB and a site on its DNA substrate showed concurrent changes in extension and FRET, suggesting that SSB can transition between different binding modes, and also FRET changes independent of changes in extension, suggesting that SSB can slide along DNA in a given binding mode. This experiment further rules out a “rolling” mechanism of diffusion. The different binding modes of SSB may be used selectively in various ssDNA maintenance processes.

Duesterberg et al. used combined optical tweezers and FRET to investigate the structure of the thiamine pyrophosphate (TPP) riboswitch [107], which controls uptake of the vitamin thiamine and is commonly repurposed in engineering control of gene expression circuits. The authors labeled two of the helix arms of the riboswitch with a FRET dye pair to monitor changes in its tertiary conformation during mechanical unfolding. They observed that the two substrate-bound state of the riboswitch – weakly-bound (requiring moderate force to unfold) and strongly-bound (requiring large force to unfold) – correlate with distinct structural arrangements of the helix arms (Figure 5C). The weakly-bound state is not able to complete the helix arm docking required for stable substrate binding. The conversion from the weakly-bound to the strongly-bound state may help discriminate between the thiamine pyrophosphate substrate and its analogs thiamine and thiamine monophosphate.

Whitley et al. used combined optical tweezers and fluorescence to probe the elasticity of ultrashort (< 15 nt) nucleic acid duplexes, which commonly serve as primers in DNA replication [108]. The binding of a labeled oligonucleotide provided an unambiguous signal which facilitated extension measurements at low forces where mechanical noise was higher. The study concluded that for these sequences edge-

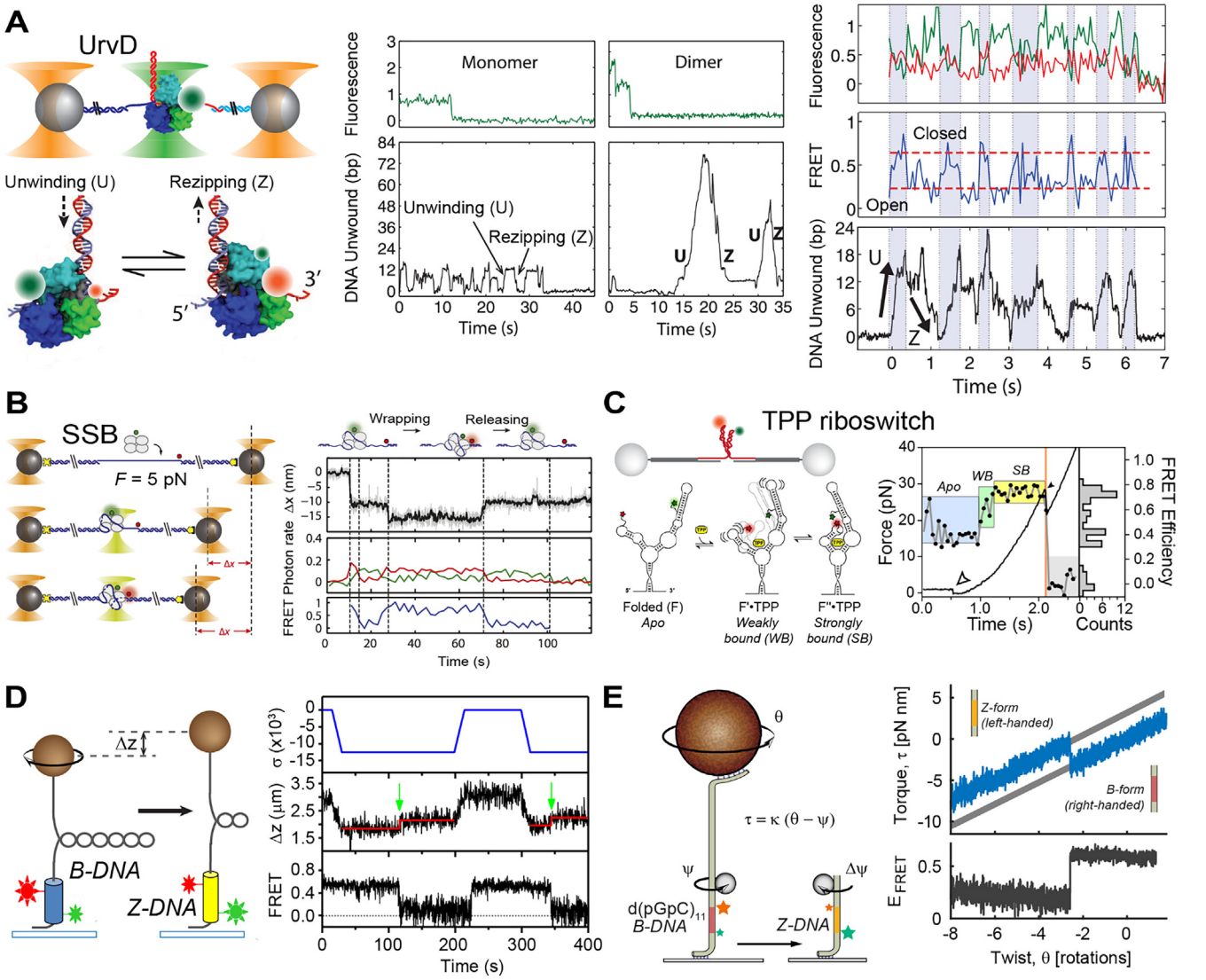

Figure 5. Multimodal measurements of conformational dynamics in nucleic acids and nucleoprotein complexes. (**A**) DNA unwinding by the UvrD helicase is governed by its oligomeric state and structural conformation [104]. Left: UvrD unwinding of a DNA hairpin was monitored via optical tweezers. UvrD monomers were labeled with a single dye or a FRET pair. Middle: Two types of unwinding activity were observed – "frustrated" and "long-distance", depending on the protein oligomeric state, inferred from the number of dye photobleaching events. Right: The Closed and Open monomer conformations correlate with DNA unwinding (U) and rezipping (Z). (**B**) Different binding modes of the single-stranded DNA binding (SSB) protein were identified by combined optical tweezers and FRET [106]. Left: SSB binding to DNA leads to wrapping of 35 nucleotides (nt) or 56 nt of DNA, as determined from the change in DNA contour length (Δx) in the optical trap. Fluorescent labels on the protein and DNA substrate allowed visualization of transitions between binding modes and identified sliding mechanisms. Right: Transition from the 35 nt to the 56 nt DNA binding mode leads to concurrent changes in FRET and DNA extension. (**C**) Combined optical tweezers and FRET identify changes in secondary and tertiary structure of the TPP riboswitch upon substrate binding [107]. Left: The two helical arms of the riboswitch were labeled with a FRET dye pair and the riboswitch was unfolded under force. Right: Changes in FRET efficiency were observed upon ligand binding and conversion from the weakly bound (WB) to the strongly bound (SB) state. Unfolding of the riboswitch in the SB state requires higher force compared to the WB state. (**D**) Transitions between B-form and Z-form DNA under controlled superhelical density (σ) were detected in combined magnetic tweezers and FRET [109]. Left: The magnetic bead was rotated under low tension to negatively supercoil the DNA. A FRET-labeled $(GC)_{11}$ repeat sequence of interest (SOI) was inserted in the DNA tether. Right: Transition of the SOI from B-form DNA to Z-form DNA relaxes some of the negative supercoils, leading to a change in the height of the magnetic bead (Δz, green arrows). At the same time, a change in FRET between the dyes incorporated in the backbone of the SOI is observed. (**E**) The same SOI as in **D** was used in FluoRBT proof-of-principle experiments [100]. Left: The applied torque (τ) was measured based on the calibrated angular deflection of the DNA segment between the magnetic bead and the rotor bead. Right: The B-Z DNA transition was detected as concurrent jump in torque and FRET efficiency. A continuous change in FRET efficiency with applied torque was also observed. Figure panels are reproduced with modification and published with permission.

dependent effects lead to deviations from the common DNA elasticity models at high forces. Helicases and other enzymes may exploit this effect to initiate DNA unwinding.

Lee et al. demonstrated the first multimodal magnetic tweezers assay combining extension measurements with FRET (Figure 5D) [109]. The authors incorporated a fluorescently-labeled GC-repeat sequence of interest in a DNA tether that underwent transitions between B-form and Z-form DNA under negative torque. The DNA tether was supercoiled by rotating the magnetic bead and at low superhelical density the B-Z transition was observed via change in FRET and concurrent change in extension of the tether due to partial relaxation of DNA plectonemes. Well-characterized structural transitions in DNA hairpins and Holliday junctions have also been used in characterization of high-resolution magnetic tweezers instrument combined with FRET [110].

Finally, rotor bead tracking (implemented in magnetic tweezers) was combined with FRET in a technique called FluoRBT (Figure 5E)

[100]. As in conventional magnetic tweezers, the magnetic bead can be used to apply force and alter the superhelical density in DNA; additionally, the rotor bead can be used to detect changes in DNA torque, twist, and extension at high resolution. Fluorescent probes on the DNA or associated nucleoproteins serve as sensitive reporters of conformational and compositional changes. Proof-of-principle experiments included unfolding a DNA hairpin under force and inducing the B-Z DNA transition under negative torque. Concurrent changes in FRET and DNA extension or torque were observed at the structural transition, as expected. FluoRBT enabled the discovery of an unanticipated continuous change in FRET with torque in both B- and Z-DNA conformations of the GC-repeat sequence, which may enable construction of molecular torque sensors, analogous to previously reported DNA-based molecular force sensors [94,111,112]. This study also illustrated how multimodal data can be used to make high-resolution FRET measurements of molecular states by post-synchronization of noisy fluorescence traces to easily identifiable mechanical events.

5. Outlook

Extending single-molecule techniques to report on multiple degrees of freedom will allow us to more faithfully capture the multidimensional dynamics of complex molecular machines. Advanced single-molecule methods such as rotor bead tracking, multicolor FRET, or multi-bead optical tweezers are powerful in extracting more information from current assays and may enable new measurements, e.g. observing DNA decatenation [113]. Combining different techniques in the same assay can leverage their individual strengths and increase the number of observable degrees of freedom [10]. Recent applications of combined magnetic tweezers or optical tweezers with fluorescence and FRET have demonstrated high-resolution measurements of conformational changes in DNA together with sensitive detection of local structural rearrangements in the proteins driving those changes.

Combining other single-molecule methods with fluorescence and FRET should, in principle, also be possible, and will allow detection of new modalities of molecular motion. Sugawa et al. recently demonstrated combined particle tracking and FRET in studying rotation of the γ shaft in the F_1-ATPase together with conformational changes in the $\alpha_3\beta_3$ stator ring [114], using an approach that might be adapted for nucleoprotein machines. The prospect of combining nanopore technology [70], acoustic force spectroscopy [45], or high-speed atomic force microscopy [115,116] with fluorescence has also been suggested. With an arsenal of next-generation single-molecule methods, we will be equipped to probe the workings of molecular machines behind central biological processes.

Acknowledgements

Funding: This work was supported in part by a Tusher Family Stanford Interdisciplinary Graduate Fellowship to I.E.I. and by National Institutes of Health grant GM106159 to Z.B.

References

[1] W.J. Greenleaf, M.T. Woodside, S.M. Block, High-resolution, single-molecule measurements of biomolecular motion, Annu. Rev. Biophys. Biomol. Struct. 36 (1) (2007) 171–190, https://doi.org/10.1146/annurev.biophys.36.101106.101451.
[2] D. Dulin, J. Lipfert, M.C. Moolman, N.H. Dekker, Studying genomic processes at the single-molecule level: introducing the tools and applications, Nat. Rev. Genet. 14 (1) (2013) 9–22, https://doi.org/10.1038/nrg3316.
[3] F.M. Fazal, S.M. Block, Optical tweezers study life under tension, Nat. Photonics 5 (2011) 318–321, https://doi.org/10.1038/nphoton.2011.100.
[4] M.T. Woodside, S.M. Block, Reconstructing folding energy landscapes by single-molecule force spectroscopy, Annu. Rev. Biophys. 43 (1) (2014) 19–39, https://doi.org/10.1146/annurev-biophys-051013-022754.
[5] E. Lerner, T. Cordes, A. Ingargiola, Y. Alhadid, S. Chung, X. Michalet, S. Weiss, Toward dynamic structural biology: two decades of single-molecule Förster resonance energy transfer, Science 359 (6373) (2018) eaan1133, https://doi.org/10.1126/science.aan1133.
[6] R. Roy, S. Hohng, T. Ha, A practical guide to single-molecule FRET, Nat. Methods 5 (6) (2008) 507–516, https://doi.org/10.1038/nmeth.1208.
[7] A.R. Dunn, J.A. Spudich, Dynamics of the unbound head during myosin V processive translocation, Nat. Struct. Mol. Biol. 14 (2007) 246, https://doi.org/10.1038/nsmb1206.
[8] M. Ohmachi, Y. Komori, A.H. Iwane, F. Fujii, T. Jin, T. Yanagida, Fluorescence microscopy for simultaneous observation of 3D orientation and movement and its application to quantum rod-tagged myosin V, Proc. Natl. Acad. Sci. U.S.A. 109 (14) (2012) 5294, https://doi.org/10.1073/pnas.1118472109.
[9] R. Yasuda, H. Noji, M. Yoshida, K. Kinosita Jr, H. Itoh, Resolution of distinct rotational substeps by submillisecond kinetic analysis of F1-ATPase, Nature 410 (2001) 898, https://doi.org/10.1038/35073513.
[10] T. Ha, Single-molecule methods leap ahead, Nat. Methods 11 (10) (2014) 1015–1018, https://doi.org/10.1038/nmeth.3107.
[11] M.H. Shabestari, A.E.C. Meijering, W.H. Roos, G.J.L. Wuite, E.J.G. Peterman, Recent advances in biological single-molecule applications of optical tweezers and fluorescence microscopy, in: M. Spies, Y.R. Chemla (Eds.), Methods in Enzymology, Academic Press, Cambridge, MA, 2017, pp. 85–119.
[12] J.C. Cordova, D.K. Das, H.W. Manning, M.J. Lang, Combining single-molecule manipulation and single-molecule detection, Curr. Opin. Struct. Biol. 28(Supplement C) (2014) 142–148, https://doi.org/10.1016/j.sbi.2014.08.010.
[13] S. Hohng, S. Lee, J. Lee, M.H. Jo, Maximizing information content of single-molecule FRET experiments: multi-color FRET and FRET combined with force or torque, Chem. Soc. Rev. 43 (4) (2014) 1007–1013, https://doi.org/10.1039/c3cs60184f.
[14] K.C. Neuman, A. Nagy, Single-molecule force spectroscopy: optical tweezers, magnetic tweezers and atomic force microscopy, Nat. Methods 5 (6) (2008) 491–505, https://doi.org/10.1038/nmeth.1218.
[15] K.D. Whitley, M.J. Comstock, Y.R. Chemla, High-resolution optical tweezers combined with single-molecule confocal microscopy, in: M. Spies, Y.R. Chemla (Eds.), Methods in Enzymology, Academic Press, Cambridge, MA, 2017, pp. 137–169.
[16] D. Dulin, T.J. Cui, J. Cnossen, Margreet W. Docter, J. Lipfert, Nynke H. Dekker, High spatiotemporal-resolution magnetic tweezers: calibration and applications for DNA dynamics, Biophys. J. 109 (10) (2015) 2113–2125, https://doi.org/10.1016/j.bpj.2015.10.018.
[17] J. Gore, Z. Bryant, M. Nöllmann, M.U. Le, N.R. Cozzarelli, C. Bustamante, DNA overwinds when stretched, Nature 442 (7104) (2006) 836–839, https://doi.org/10.1038/nature04974.
[18] Z. Bryant, M.D. Stone, J. Gore, S.B. Smith, N.R. Cozzarelli, C. Bustamante, Structural transitions and elasticity from torque measurements on DNA, Nature 424 (6946) (2003) 338–341, https://doi.org/10.1038/nature01810.
[19] Z. Bryant, F.C. Oberstrass, A. Basu, Recent developments in single-molecule DNA mechanics, Curr. Opin. Struct. Biol. 22 (3) (2012) 304–312, https://doi.org/10.1016/j.sbi.2012.04.007.
[20] J.C. Wang, Cellular roles of DNA topoisomerases: a molecular perspective, Nat. Rev. Mol. Cell. Biol. 3 (6) (2002) 430–440, https://doi.org/10.1038/nrm831.
[21] Y. Harada, O. Ohara, A. Takatsuki, H. Itoh, N. Shimamoto, K. Kinosita Jr, Direct observation of DNA rotation during transcription by Escherichia coli RNA polymerase, Nature 409 (2001) 113, https://doi.org/10.1038/35051126.
[22] E.A. Abbondanzieri, W.J. Greenleaf, J.W. Shaevitz, R. Landick, S.M. Block, Direct observation of base-pair stepping by RNA polymerase, Nature 438 (7067) (2005) 460–465, https://doi.org/10.1038/nature04268.
[23] A. Basu, A.J. Schoeffler, J.M. Berger, Z. Bryant, ATP binding controls distinct structural transitions of Escherichia coli DNA gyrase in complex with DNA, Nat. Struct. Mol. Biol. 19 (5) (2012) 538–546, https://doi.org/10.1038/nsmb.2278.
[24] P. Lebel, A. Basu, F.C. Oberstrass, E.M. Tretter, Z. Bryant, Gold rotor bead tracking for high-speed measurements of DNA twist, torque and extension, Nat. Methods 11 (4) (2014) 456–462, https://doi.org/10.1038/nmeth.2854.
[25] F.C. Oberstrass, L.E. Fernandes, Z. Bryant, Torque measurements reveal sequence-specific cooperative transitions in supercoiled DNA, Proc. Natl. Acad. Sci. U.S.A. 109 (16) (2012) 6106–6111, https://doi.org/10.1073/pnas.1113532109.
[26] F.C. Oberstrass, L.E. Fernandes, P. Lebel, Z. Bryant, Torque spectroscopy of DNA: base-pair stability, boundary effects, backbending, and breathing dynamics, Phys. Rev. Lett. 110 (17) (2013) 178103, , https://doi.org/10.1103/PhysRevLett. 110.178103.
[27] A. Basu, M. Hobson, P. Lebel, L.E. Fernandes, E.M. Tretter, J.M. Berger, Z. Bryant, Dynamic coupling between conformations and nucleotide states in DNA gyrase, Nat. Chem. Biol. 14 (6) (2018) 565–574, https://doi.org/10.1038/s41589-018-0037-0.
[28] J. Lipfert, M. Wiggin, J.W.J. Kerssemakers, F. Pedaci, N.H. Dekker, Freely orbiting magnetic tweezers to directly monitor changes in the twist of nucleic acids, Nat. Commun. 2 (2011) 439, https://doi.org/10.1038/ncomms1450.
[29] J. Lipfert, J.W.J. Kerssemakers, T. Jager, N.H. Dekker, Magnetic torque tweezers: measuring torsional stiffness in DNA and RecA-DNA filaments, Nat. Methods 7 (12) (2010) 977–980, https://doi.org/10.1038/nmeth.1520.
[30] X.J.A. Janssen, J. Lipfert, T. Jager, R. Daudey, J. Beekman, N.H. Dekker, Electromagnetic torque tweezers: a versatile approach for measurement of single-molecule twist and torque, Nano Lett. 12 (7) (2012) 3634–3639, https://doi.org/10.1021/nl301330h.
[31] A. La Porta, M.D. Wang, Optical torque wrench: angular trapping, rotation, and torque detection of quartz microparticles, Phys. Rev. Lett. 92 (19) (2004) 190801, , https://doi.org/10.1103/PhysRevLett. 92.190801.
[32] J. Gore, Z. Bryant, M.D. Stone, M. Nöllmann, N.R. Cozzarelli, C. Bustamante, Mechanochemical analysis of DNA gyrase using rotor bead tracking, Nature 439 (2006) 100, https://doi.org/10.1038/nature04319.

[33] S. Liu, G. Chistol, Craig L. Hetherington, S. Tafoya, K. Aathavan, J. Schnitzbauer, S. Grimes, Paul J. Jardine, C. Bustamante, A Viral packaging motor varies its DNA rotation and step size to preserve subunit coordination as the capsid fills, Cell (157(3), 2014,) 702–713, https://doi.org/10.1016/j.cell.2014.02.034.
[34] J. Ma, L. Bai, M.D. Wang, Transcription under torsion, Science 340 (6140) (2013) 1580, https://doi.org/10.1126/science.1235441.
[35] I. Heller, N. Laurens, D. Vorselen, O.D. Broekmans, A.S. Biebricher, G.A. King, I. Brouwer, G.J.L. Wuite, E.J.G. Peterman, Versatile quadruple-trap optical tweezers for dual DNA experiments, in: A. Gennerich (Ed.), Optical Tweezers, Methods in Molecular Biology, Springer, New York, New York, NY, 2017, pp. 257–272.
[36] M.C. Noom, B. van den Broek, J. van Mameren, G.J.L. Wuite, Visualizing single DNA-bound proteins using DNA as a scanning probe, Nat. Methods 4 (2007) 1031, https://doi.org/10.1038/nmeth1126.
[37] R.T. Dame, M.C. Noom, G.J.L. Wuite, Bacterial chromatin organization by H-NS protein unravelled using dual DNA manipulation, Nature 444 (2006) 387, https://doi.org/10.1038/nature05283.
[38] N.A. Kurniawan, B.E. Vos, A. Biebricher, G.J.L. Wuite, E.J.G. Peterman, G.H. Koenderink, Fibrin networks support recurring mechanical loads by adapting their structure across multiple scales, Biophys. J. 111 (5) (2016) 1026–1034, https://doi.org/10.1016/j.bpj.2016.06.034.
[39] I. De Vlaminck, T. Henighan, M.T.J. van Loenhout, I. Pfeiffer, J. Huijts, J.W.J. Kerssemakers, A.J. Katan, A. van Langen-Suurling, E. van der Drift, C. Wyman, C. Dekker, Highly parallel magnetic tweezers by targeted DNA tethering, Nano Lett. 11 (12) (2011) 5489–5493, https://doi.org/10.1021/nl203299e.
[40] M. Soltani, J. Lin, R.A. Forties, J.T. Inman, S.N. Saraf, R.M. Fulbright, M. Lipson, M.D. Wang, Nanophotonic trapping for precise manipulation of biomolecular arrays, Nat. Nanotechnol. 9 (2014) 448, https://doi.org/10.1038/nnano.2014.79.
[41] J.E. Baker, R.P. Badman, M.D. Wang, Nanophotonic trapping: precise manipulation and measurement of biomolecular arrays, Wiley Interdiscip.Rev.: Nanomed. Nanobiotechnol. 10 (1) (2018) e1477, https://doi.org/10.1002/wnan.1477.
[42] D.G. Grier, Y. Roichman, Holographic optical trapping, Appl. Opt. 45 (5) (2006) 880–887, https://doi.org/10.1364/AO.45.000880.
[43] A. Farré, A. van der Horst, G.A. Blab, B.P.B. Downing, N.R. Forde, Stretching single DNA molecules to demonstrate high-force capabilities of holographic optical tweezers, J. Biophotonics 3 (4) (2010) 224–233, https://doi.org/10.1002/jbio.200900107.
[44] G. Sitters, D. Kamsma, G. Thalhammer, M. Ritsch-Marte, E.J.G. Peterman, G.J.L. Wuite, Acoustic force spectroscopy, Nat. Methods 12 (2014) 47–50, https://doi.org/10.1038/nmeth.3183.
[45] D. Kamsma, R. Creyghton, G. Sitters, G.J.L. Wuite, E.J.G. Peterman, Tuning the music: acoustic force spectroscopy (AFS) 2.0, Methods 105 (2016) 26–33, https://doi.org/10.1016/j.ymeth.2016.05.002.
[46] K. Halvorsen, W.P. Wong, Massively parallel single-molecule manipulation using centrifugal force, Biophys. J. 98 (11) (2010) L53–L55, https://doi.org/10.1016/j.bpj.2010.03.012.
[47] G. Thalhammer, R. Steiger, M. Meinschad, M. Hill, S. Bernet, M. Ritsch-Marte, Combined acoustic and optical trapping, Biomed. Opt. Express 2 (10) (2011) 2859–2870, https://doi.org/10.1364/BOE.2.002859.
[48] I. De Vlaminck, T.J. van Marijn, L. Loenhout, J. den Zweifel, K. Blanken, S. Hooning, J. Hage, C. Dekker Kerssemakers, Mechanism of homology recognition in DNA recombination from dual-molecule experiments, Mol. Cell 46 (5) (2012) 616–624, https://doi.org/10.1016/j.molcel.2012.03.029.
[49] S. Lee, Y. Jang, S.J. Lee, S. Hohng, Single-molecule multicolor FRET assay for studying structural dynamics of biomolecules, in: M. Spies, Y.R. Chemla (Eds.), Methods in Enzymology, Academic Press, Cambridge, MA, 2016, pp. 461–486.
[50] M. Götz, P. Wortmann, S. Schmid, T. Hugel, A multicolor single-molecule FRET approach to study protein dynamics and interactions simultaneously, in: M. Spies, Y.R. Chemla (Eds.), Methods in Enzymology, Academic Press, Cambridge, MA, 2016, pp. 487–516.
[51] S. Hohng, C. Joo, T. Ha, Single-molecule three-color FRET, Biophys. J. 87 (2) (2004) 1328–1337, https://doi.org/10.1529/biophysj.104.043935.
[52] S. Lee, J. Lee, S. Hohng, Single-molecule three-color fret with both negligible spectral overlap and long observation time, PLoS One 5 (8) (2010) e12270, , https://doi.org/10.1371/journal.pone.0012270.
[53] N.K. Lee, A.N. Kapanidis, H.R. Koh, Y. Korlann, S.O. Ho, Y. Kim, N. Gassman, S.K. Kim, S. Weiss, Three-color alternating-laser excitation of single molecules: monitoring multiple interactions and distances, Biophys. J. 92 (1) (2007) 303–312, https://doi.org/10.1529/biophysj.106.093211.
[54] J. Ross, P. Buschkamp, D. Fetting, A. Donnermeyer, C.M. Roth, P. Tinnefeld, Multicolor single-molecule spectroscopy with alternating laser excitation for the investigation of interactions and dynamics, J. Phys. Chem. B 111 (2) (2007) 321–326, https://doi.org/10.1021/jp066082g.
[55] J. Lee, S. Lee, K. Ragunathan, C. Joo, T. Ha, S. Hohng, Single-molecule four-color FRET, Angew. Chem., Int. Ed. 49 (51) (2010) 9922–9925, https://doi.org/10.1002/anie.201005402.
[56] J.B. Munro, R.B. Altman, C.-S. Tung, J.H.D. Cate, K.Y. Sanbonmatsu, S.C. Blanchard, Spontaneous formation of the unlocked state of the ribosome is a multistep process, Proc. Natl. Acad. Sci. U.S.A. 107 (2) (2010) 709, https://doi.org/10.1073/pnas.0908597107.
[57] H. Kim, S.C. Abeysirigunawarden, K. Chen, M. Mayerle, K. Ragunathan, Z. Luthey-Schulten, T. Ha, S.A. Woodson, Protein-guided RNA dynamics during early ribosome assembly, Nature 506 (2014) 334, https://doi.org/10.1038/nature13039.
[58] R. Roy, A.G. Kozlov, T.M. Lohman, T. Ha, SSB protein diffusion on single-stranded DNA stimulates RecA filament formation, Nature 461 (2009) 1092, https://doi.org/10.1038/nature08442.
[59] S. Lee, S. Hohng, An optical trap combined with three-color FRET, J. Am. Chem. Soc. 135 (49) (2013) 18260–18263, https://doi.org/10.1021/ja408767p.
[60] M.J. Levene, J. Korlach, S.W. Turner, M. Foquet, H.G. Craighead, W.W. Webb, Zero-mode waveguides for single-molecule analysis at high concentrations, Science 299 (5607) (2003) 682, https://doi.org/10.1126/science.1079700.
[61] J. Eid, A. Fehr, J. Gray, K. Luong, J. Lyle, G. Otto, P. Peluso, D. Rank, P. Baybayan, B. Bettman, A. Bibillo, K. Bjornson, B. Chaudhuri, F. Christians, R. Cicero, S. Clark, R. Dalal, A. deWinter, J. Dixon, M. Foquet, A. Gaertner, P. Hardenbol, C. Heiner, K. Hester, D. Holden, G. Kearns, X. Kong, R. Kuse, Y. Lacroix, S. Lin, P. Lundquist, C. Ma, P. Marks, M. Maxham, D. Murphy, I. Park, T. Pham, M. Phillips, J. Roy, R. Sebra, G. Shen, J. Sorenson, A. Tomaney, K. Travers, M. Trulson, J. Vieceli, J. Wegener, D. Wu, A. Yang, D. Zaccarin, P. Zhao, F. Zhong, J. Korlach, S. Turner, Real-time DNA sequencing from single polymerase molecules, Science 323 (5910) (2009) 133–138, https://doi.org/10.1126/science:1162986.
[62] P. Zhu, H.G. Craighead, Zero-mode waveguides for single-molecule analysis, Annu. Rev. Biophys. 41 (1) (2012) 269–293, https://doi.org/10.1146/annurev-biophys-050511-102338.
[63] S. Uemura, C.E. Aitken, J. Korlach, B.A. Flusberg, S.W. Turner, J.D. Puglisi, Real-time tRNA transit on single translating ribosomes at codon resolution, Nature 464 (2010) 1012, https://doi.org/10.1038/nature08925.
[64] A. Tsai, J.D. Puglisi, S. Uemura, Probing the translation dynamics of ribosomes using zero-mode waveguides, in: S. Yoshizawa (Ed.), Progress in Molecular Biology and Translational Science, Academic Press, Cambridge, MA, 2016, pp. 1–43.
[65] S.R. Leslie, A.P. Fields, A.E. Cohen, convex lens-induced confinement for imaging single molecules, Anal. Chem. 82 (14) (2010) 6224–6229, https://doi.org/10.1021/ac101041s.
[66] S. Scott, Zhi M. Xu, F. Kouzine, D.J. Berard, C. Shaheen, B. Gravel, L. Saunders, A. Hofkirchner, C. Leroux, J. Laurin, D. Levens, C.J. Benham, S.R. Leslie, Visualizing structure-mediated interactions in supercoiled DNA molecules, Nucleic Acids Res. 46 (9) (2018) 4622–4631, https://doi.org/10.1093/nar/gky266.
[67] A.H. Laszlo, I.M. Derrington, J.H. Gundlach, MspA nanopore as a single-molecule tool: from sequencing to SPRNT, Methods 105 (2016) 75–89, https://doi.org/10.1016/j.ymeth.2016.03.026.
[68] K. Willems, V. Van Meervelt, C. Wloka, G. Maglia, Single-molecule nanopore enzymology, Philos Trans. R. Soc., B 372 (1726) (2017) 20160230, https://doi.org/10.1098/rstb.2016.0230.
[69] A.H. Squires, T. Gilboa, C. Torfstein, N. Varongchayakul, A. Meller, Single-molecule characterization of DNA–protein interactions using nanopore biosensors, in: M. Spies, Y.R. Chemla (Eds.), Methods in Enzymology, Academic Press, Cambridge, MA, 2017, pp. 353–385.
[70] A.H. Laszlo, I.M. Derrington, J.H. Gundlach, Subangstrom measurements of enzyme function using a biological nanopore, SPRNT, in: M. Spies, Y.R. Chemla (Eds.), Methods in Enzymology, Academic Press, Cambridge, MA, 2017, pp. 387–414.
[71] G.M. Cherf, K.R. Lieberman, H. Rashid, C.E. Lam, K. Karplus, M. Akeson, Automated forward and reverse ratcheting of DNA in a nanopore at 5-Å precision, Nat. Biotechnol. 30 (2012) 344, https://doi.org/10.1038/nbt.2147.
[72] E.A. Manrao, I.M. Derrington, A.H. Laszlo, K.W. Langford, M.K. Hopper, N. Gillgren, M. Pavlenok, M. Niederweis, J.H. Gundlach, Reading DNA at single-nucleotide resolution with a mutant MspA nanopore and phi29 DNA polymerase, Nat. Biotechol. 30 (4) (2012) 349–353, https://doi.org/10.1038/nbt.2171.
[73] K.R. Lieberman, J.M. Dahl, A.H. Mai, M. Akeson, H. Wang, Dynamics of the translocation step measured in individual DNA polymerase complexes, J. Am. Chem. Soc. 134 (45) (2012) 18816–18823, https://doi.org/10.1021/ja3090302.
[74] K.R. Lieberman, J.M. Dahl, A.H. Mai, A. Cox, M. Akeson, H. Wang, Kinetic mechanism of translocation and dNTP binding in individual DNA polymerase complexes, J. Am. Chem. Soc. 135 (24) (2013) 9149–9155, https://doi.org/10.1021/ja403640b.
[75] I.M. Derrington, J.M. Craig, E. Stava, A.H. Laszlo, B.C. Ross, H. Brinkerhoff, I.C. Nova, K. Doering, B.I. Tickman, M. Ronaghi, J.G. Mandell, K.L. Gunderson, J.H. Gundlach, Subangstrom single-molecule measurements of motor proteins using a nanopore, Nat. Biotechnol. 33 (2015) 1073, https://doi.org/10.1038/nbt.3357.
[76] J.M. Craig, A.H. Laszlo, H. Brinkerhoff, I.M. Derrington, M.T. Noakes, I.C. Nova, B.I. Tickman, K. Doering, N.F. de Leeuw, J.H. Gundlach, Revealing dynamics of helicase translocation on single-stranded DNA using high-resolution nanopore tweezers, Proc. Natl. Acad. Sci. U.S.A. 114 (45) (2017) 11932, https://doi.org/10.1073/pnas.1711282114.
[77] I.C. Nova, A. Mazumder, J.M. Craig, A.H. Laszlo, I.M. Derrington, M.T. Noakes, H. Brinkerhoff, J. Bowman, J.W. Mount, B.I. Tickman, R.H. Ebright, J.H. Gundlach, Nanopore tweezers reveal detailed RNA polymerase dynamics at a sequence-specific pause element, Biophys. J. 114 (3) (2018) 193a, https://doi.org/10.1016/j.bpj.2017.11.1077.
[78] S. Sorgenfrei, C.-Y. Chiu, R.L. Gonzalez Jr, Y.-J. Yu, P. Kim, C. Nuckolls, K.L. Shepard, Label-free single-molecule detection of DNA-hybridization kinetics with a carbon nanotube field-effect transistor, Nat. Nanotechnol. 6 (2011) 126, https://doi.org/10.1038/nnano.2010.275.
[79] Y. Choi, I.S. Moody, P.C. Sims, S.R. Hunt, B.L. Corso, I. Perez, G.A. Weiss, P.G. Collins, Single-molecule lysozyme dynamics monitored by an electronic circuit, Science 335 (6066) (2012) 319, https://doi.org/10.1126/science.1214824.
[80] M.A. van Dijk, L.C. Kapitein, J. van Mameren, C.F. Schmidt, E.J.G. Peterman, Combining optical trapping and single-molecule fluorescence spectroscopy: enhanced photobleaching of fluorophores, J. Phys. Chem. B 108 (20) (2004) 6479–6484, https://doi.org/10.1021/jp049805+.
[81] R.R. Brau, P.B. Tarsa, J.M. Ferrer, P. Lee, M.J. Lang, Interlaced optical force-

fluorescence measurements for single molecule biophysics, Biophys. J. 91 (3) (2006) 1069–1077, https://doi.org/10.1529/biophysj.106.082602.
[82] Y. Harada, T. Funatsu, K. Murakami, Y. Nonoyama, A. Ishihama, T. Yanagida, Single-molecule imaging of RNA polymerase-DNA interactions in real time, Biophys. J. 76 (2) (1999) 709–715, https://doi.org/10.1016/S0006-3495(99)77237-1.
[83] M.J. Lang, P.M. Fordyce, A.M. Engh, K.C. Neuman, S.M. Block, Simultaneous, coincident optical trapping and single-molecule fluorescence, Nat. Methods 1 (2) (2004) 133–139, https://doi.org/10.1038/nmeth714.
[84] P.B. Tarsa, R.R. Brau, M. Barch, J.M. Ferrer, Y. Freyzon, P. Matsudaira, M.J. Lang, Detecting force-induced molecular transitions with fluorescence resonant energy transfer, Angew. Chem., Int. Ed. 46 (12) (2007) 1999–2001, https://doi.org/10.1002/anie.200604546.
[85] S. Hohng, R. Zhou, M.K. Nahas, J. Yu, K. Schulten, D.M.J. Lilley, T. Ha, Fluorescence-force spectroscopy maps two-dimensional reaction landscape of the holliday junction, Science 318 (5848) (2007) 279–283, https://doi.org/10.1126/science.1146113.
[86] R. Zhou, Alexander G. Kozlov, R. Roy, J. Zhang, S. Korolev, Timothy M. Lohman, T. Ha, SSB functions as a sliding platform that migrates on DNA via reptation, Cell 146 (2) (2011) 222–232, https://doi.org/10.1016/j.cell.2011.06.036.
[87] Thuy T.M. Ngo, Q. Zhang, R. Zhou, Jaya G. Yodh, T. Ha, Asymmetric unwrapping of nucleosomes under tension directed by DNA local flexibility, Cell 160 (6) (2015) 1135–1144, https://doi.org/10.1016/j.cell.2015.02.001.
[88] A. Candelli, G.J.L. Wuite, E.J.G. Peterman, Combining optical trapping, fluorescence microscopy and micro-fluidics for single molecule studies of DNA-protein interactions, Phys. Chem. Chem. Phys. 13 (16) (2011) 7263–7272, https://doi.org/10.1039/c0cp02844d.
[89] J. van Mameren, P. Gross, G. Farge, P. Hooijman, M. Modesti, M. Falkenberg, G.J.L. Wuite, E.J.G. Peterman, Unraveling the structure of DNA during overstretching by using multicolor, single-molecule fluorescence imaging, Proc. Natl. Acad. Sci. U.S.A. 106 (43) (2009) 18231.
[90] K. Schakenraad, A.S. Biebricher, M. Sebregts, B. ten Bensel, E.J.G. Peterman, G.J.L. Wuite, I. Heller, C. Storm, P. van der Schoot, Hyperstretching DNA, Nat. Commun. 8 (2017) 2197, https://doi.org/10.1038/s41467-017-02396-1.
[91] G.A. King, E.J.G. Peterman, G.J.L. Wuite, Unravelling the structural plasticity of stretched DNA under torsional constraint, Nat. Commun. 7 (2016) 11810, https://doi.org/10.1038/ncomms11810.
[92] M.D. Newton, B.J. Taylor, R.P.C. Driessen, L. Roos, N. Cvetesic, S. Allyjaun, B. Lenhard, M.E. Cuomo, D.S. Rueda, DNA stretching induces Cas9 off-target activity, Nat. Struct. Mol. Biol. 26 (3) (2019) 185–192, https://doi.org/10.1038/s41594-019-0188-z.
[93] X. Long, J.W. Parks, M.D. Stone, Integrated magnetic tweezers and single-molecule FRET for investigating the mechanical properties of nucleic acid, Methods 105 (2016) 16–25, https://doi.org/10.1016/j.ymeth.2016.06.009.
[94] H. Shroff, B.M. Reinhard, M. Siu, H. Agarwal, A. Spakowitz, J. Liphardt, Biocompatible force sensor with optical readout and dimensions of 6 nm(3), Nano Lett. 5 (7) (2005) 1509–1514, https://doi.org/10.1021/nl050875h.
[95] X. Long, J.W. Parks, C.R. Bagshaw, M.D. Stone, Mechanical unfolding of human telomere G-quadruplex DNA probed by integrated fluorescence and magnetic tweezers spectroscopy, Nucleic Acids Res. 41 (4) (2013) 2746–2755, https://doi.org/10.1093/nar/gks1341.
[96] M.J. Comstock, T. Ha, Y.R. Chemla, Ultrahigh-resolution optical trap with single-fluorophore sensitivity, Nat. Methods 8 (4) (2011) 335–340, https://doi.org/10.1038/nmeth.1574.
[97] J.R. Moffitt, Y.R. Chemla, D. Izhaky, C. Bustamante, Differential detection of dual traps improves the spatial resolution of optical tweezers, Proc. Natl. Acad. Sci. U.S.A. 103 (24) (2006) 9006, https://doi.org/10.1073/pnas.0603342103.
[98] K.D. Whitley, M.J. Comstock, Y.R. Chemla, High-resolution “Fleezers”: dual-trap optical tweezers combined with single-molecule fluorescence detection, in: A. Gennerich (Ed.), Optical Tweezers, Humana Press, New York, NY, Methods in Molecular Biology, 2017, pp. 183–256.
[99] F.E. Kemmerich, K. Kasaciunaite, R. Seidel, Modular magnetic tweezers for single-molecule characterizations of helicases, Methods 108 (2016) 4–13, https://doi.org/10.1016/j.ymeth.2016.07.004.
[100] I.E. Ivanov, P. Lebel, F.C. Oberstrass, C.H. Starr, A.C. Parente, A. Ierokomos, Z. Bryant, Multimodal measurements of single-molecule dynamics using FluoRBT, Biophys. J. 114 (2) (2018) 278–282, https://doi.org/10.1016/j.bpj.2017.11.017.
[101] A. Huhle, D. Klaue, H. Brutzer, P. Daldrop, S. Joo, O. Otto, U.F. Keyser, R. Seidel, Camera-based three-dimensional real-time particle tracking at kHz rates and Ångström accuracy, Nat. Commun. 6 (2015) 5885, https://doi.org/10.1038/ncomms6885.
[102] Y. Seol, K.C. Neuman, Combined magnetic tweezers and micro-mirror total internal reflection fluorescence microscope for single-molecule manipulation and visualization, in: E.J.G. Peterman (Ed.), Single Molecule Analysis, Methods in Molecular Biology, Springer, New York, New York, NY, 2018, pp. 297–316.
[103] Lumicks, C-Trap Optical Tweezers Fluorescence & Label-free Microscopy. https://lumicks.com/products/c-trap-optical-tweezers-fluorescence-label-free-microscopy/ (accessed 06/01/19).
[104] M.J. Comstock, K.D. Whitley, H. Jia, J. Sokoloski, T.M. Lohman, T. Ha, Y.R. Chemla, Direct observation of structure-function relationship in a nucleic acid–processing enzyme, Science 348 (6232) (2015) 352–354, https://doi.org/10.1126/science.aaa0130.
[105] N.K. Maluf, C.J. Fischer, T.M. Lohman, A dimer of Escherichia coli UvrD is the active form of the helicase in vitro, J. Mol. Biol. 325 (5) (2003) 913–935, https://doi.org/10.1016/S0022-2836(02)01277-9.
[106] S. Suksombat, R. Khafizov, A.G. Kozlov, T.M. Lohman, Y.R. Chemla, Structural dynamics of E. coli single-stranded DNA binding protein reveal DNA wrapping and unwrapping pathways, eLife (4) (2015) e08193, https://doi.org/10.7554/eLife.08193.
[107] V.K. Duesterberg, I.T. Fischer-Hwang, C.F. Perez, D.W. Hogan, S.M. Block, Observation of long-range tertiary interactions during ligand binding by the TPP riboswitch aptamer, eLife 4 (2015) e12362, https://doi.org/10.7554/eLife.12362.
[108] K.D. Whitley, M.J. Comstock, Y.R. Chemla, Ultrashort nucleic acid duplexes exhibit long wormlike chain behavior with force-dependent edge effects, Phys. Rev. Lett. 120 (6) (2018) 68102, https://doi.org/10.1103/PhysRevLett.120.068102.
[109] M. Lee, S.H. Kim, S.C. Hong, Minute negative superhelicity is sufficient to induce the B-Z transition in the presence of low tension, Proc. Natl. Acad. Sci. U.S.A. 107 (11) (2010) 4985–4990, https://doi.org/10.1073/pnas.0911528107.
[110] F.E. Kemmerich, M. Swoboda, D.J. Kauert, M.S. Grieb, S. Hahn, F.W. Schwarz, R. Seidel, M. Schlierf, Simultaneous single-molecule force and fluorescence sampling of DNA nanostructure conformations using magnetic tweezers, Nano Lett. 16 (1) (2016) 381–386, https://doi.org/10.1021/acs.nanolett.5b03956.
[111] Y. Zhang, C. Ge, C. Zhu, K. Salaita, DNA-based digital tension probes reveal integrin forces during early cell adhesion, Nat. Commun. 5 (2014) 5167, https://doi.org/10.1038/ncomms6167.
[112] X. Wang, T. Ha, Defining single molecular forces required to activate integrin and notch signaling, Science 340 (6135) (2013) 991, https://doi.org/10.1126/science.1231041.
[113] K. Yogo, T. Ogawa, M. Hayashi, Y. Harada, T. Nishizaka, K. Kinosita Jr., Direct observation of strand passage by DNA-topoisomerase and its limited processivity, PLoS One 7 (4) (2012) e34920, , https://doi.org/10.1371/journal.pone.0034920.
[114] M. Sugawa, K.-I. Okazaki, M. Kobayashi, T. Matsui, G. Hummer, T. Masaike, T. Nishizaka, F1-ATPase conformational cycle from simultaneous single-molecule FRET and rotation measurements, Proc. Natl. Acad. Sci. U.S.A. 113 (21) (2016) E2916–E2924, https://doi.org/10.1073/pnas.1524720113.
[115] S. Fukuda, T. Uchihashi, R. Iino, Y. Okazaki, M. Yoshida, K. Igarashi, T. Ando, High-speed atomic force microscope combined with single-molecule fluorescence microscope, Rev. Sci. Instrum. 84 (7) (2013) 073706, , https://doi.org/10.1063/1.4813280.
[116] T. Umakoshi, S. Fukuda, R. Iino, T. Uchihashi, T. Ando, High-speed near-field fluorescence microscopy combined with high-speed atomic force microscopy for biological studies, Biochim. Biophys. Acta, Gen. Subj. (2019), https://doi.org/10.1016/j.bbagen.2019.03.011 in press.